[Frontiers in Bioscience E3, 22-32, January 1, 2011]

EGFR activation monitored by SW-FCCS in live cells

Xiaoxiao Ma[1], Sohail Ahmed[2], Thorsten Wohland[1]

[1]Department of Chemistry, National University of Singapore, 3 Science Drive 3, Singapore 117543, [2]Institute of Medical Biology, 8A Biomedical Grove, Singapore 138665

TABLE OF CONTENTS

1. ABSTRACT

Single wavelength fluorescence cross-correlation spectroscopy (SW-FCCS) has been applied to the quantitative determination of molecular interactions at equilibrium for different molecular systems *in vitro* and *in vivo*, including living cells and organisms. Here we report for the first time the measurement of an activation and time dependent interaction between a cytosolic and a membrane bound protein by SW-FCCS in live cells. On the example of the epidermal growth factor (EGF) receptor (EGFR) we confirm the existence of pre-formed dimers in the absence of stimulation and demonstrate that the activation of the receptor can be detected by the phosphorylation dependent binding of a phosphotyrosine binding (PTB) domain. SW-FCCS results indicate that in CHO cells there is low specific interaction between PTB and EGFR, possibly indicating a low level of EGFR phosphorylation even in the absence of EGF stimulation. After EGF stimulation the interaction between PTB and EGFR increases significantly in a time dependent manner.

2. INTRODUCTION

The Epidermal Growth Factor Receptor (EGFR or ErbB1) is a tyrosine kinase that plays a fundamental role in a large variety of physiological functions in cells. The receptors of the ErbB family, including EGFR, have been associated with different cancers and been the hot-spot of drug designs (1-4). As a transmembrane receptor, EGFR transduces signals into cells and starts various signaling cascades through extracellular binding of epidermal growth factor (EGF) and EGF-like growth factors (1, 3, 5, 6). The binding domains of EGFR include phosphotyrosine-binding (PTB) domain and Src Homology 2 (SH2) domain (3). Nowadays more and more studies about membrane receptors began to focus on physiological environment. By fluorescence lifetime measurements, Verveer *et al.* have studied the spatial distribution of EGFR phosphorylation process in fixed cells (7). But a more complete understanding of EGFR stimulation requires quantitative biophysical data about its dynamics in physiological environments temporally during activation and interaction.

In the past, we have investigated the existence of pre-formed EGFR dimers before EGF stimulation. Using Single Wavelength Fluorescence Cross-Correlation Spectroscopy (SW-FCCS) we were able to show that a majority of receptor, at least 2/3, are in pre-formed dimmers (8) which is consistent with other recent reports (9-11). In this paper, we extend the investigation to the observation in time by SW-FCCS of binding of cytosolic PTB-EGFP to mRFP-EGFR after EGF stimulation and phosphorylation.

Single Wavelength Fluorescence Cross-Correlation Spectroscopy (SW-FCCS) is a versatile technique for the quantitation of protein-protein interactions in live cells (12, 13). It is derived from Fluorescence Cross-Correlation Spectroscopy (FCCS) which observes the fluorescence fluctuations form a small observation volume (~fl) of different fluorescently labelled molecules simultaneously. By cross-correlating the signal FCCS can determine whether and how many molecules of the two species interact. Usually FCCS is performed by using either two or more lasers for the one-photon excitation of the two (or more) labels or a pulsed IR laser for the simultaneous two-photon excitation of all fluorophores. SW-FCCS uses only one laser for the one-photon excitation of different fluorophores. This has the advantage of an easy and low cost implementation which avoids the more difficult alignment of multiple lasers to one single observation volume and does not need the higher cost pulsed IR lasers. SW-FCCS has been demonstrated to work with a range of fluorophore pairs including fluorescent proteins. Using green fluorescent protein (GFP) (14) and monomeric red fluorescent protein (mRFP) (15) SW-FCCS was used to determine dissociation constants in live cells and organisms (16, 17) and to quantify the dimerization of membrane proteins under physiological expression levels (8).

In this paper, we extend the use of Single Wavelength Fluorescence Cross-Correlation Spectroscopy (SW-FCCS) from the detection of EGFR-FP dimers before activation to monitoring the binding of PTB-EGFP to mRFP-EGFR after activation. EGFR has been shown to exist in dimers before stimulation to an extent of at least 2/3 of the total receptor population (8). Our previous measurements were done in a membrane receptor population at equilibrium and without EGF stimulation. Here we observe changes in PTB-EGFP/mRFP-EGFR interaction, i.e. the interaction of a cytosolic protein with a membrane receptor, over time after stimulation. The cytosolic concentration of PTB-EGFP exceeds the concentration of mRFP-EGFR on the membrane and thus the cross-correlation does not reach its possible maximum. However, the results of SW-FCCS are supported by changes in diffusion coefficients of PTB-EGFP upon binding and by a change in the ratio of the concentrations of fast cytosolic PTB-EGFP versus slow membrane bound PTB-EGFP. The measurements indicate that only a small fraction of PTB-EGFP is bound on the membrane before stimulation but that binding increases shortly after stimulation with EGF and reach a maximum after about 20-30 minutes. This is the first time that SW-FCCS was used to monitor the activation of a protein over time and demonstrates that quantitation by SW-FCCS is a promising tool for the investigation of biomolecular interaction *in vivo*.

3. MATERIALS AND METHODS

3.1. Construction of plasmids encoding chimeras between EGFR and FPs

The construction of the following plasmids has been described in a previous publication (8), in which how pEGFP-N1/PMT-mRFP, pECFP-N1/PMT-EGFP, pEGFP-N1/EGFR-EGFP constructed are shown. And pNUT/mRFP-EGFR, pNUT/mRFP-EGFR-EGFP are both initially from pNUT/EGFR plasmid which encodes human egfr cDNA (10). pcDNA3.1/PTB-citrine encoding the phosphotyrosine-binding domain from human SHC (Src homology 2 domain containing) cDNA, a gift from Dr. Philippe I. H. Bastiaens (18), is digested by BamH I and Xba I; the GFP fragment was amplified by polymerase chain reaction (PCR) from pEGFP-N1 vector (Clontech, USA) with the following oligonucleotide primers encoding BamH I and Xba I sites (underlined), respectively: 5'-CGCGGATCCATGGTGAGCAAGGGCGA and 5'-TTATGATCTAGAGTCGCGGCCGC (Sigma-Proligo, Sg Pty Ltd). The resulting PCR fragment was digested with BamH I and Xba I, and cloned into pcDNA3.1 mentioned above to make the plasmid construct encoding PTB-EGFP.

3.2. Cell culture and expression of proteins with FP

CHO-K1 (Chinese hamster ovary) cells obtained from ATCC (Manassas, VA, USA) were cultivated in Ham's F12 medium (with Kaighn's modification. Invitrogen Singapore Pte Ltd, SG) supplemented with 1% PS, penicillin G and streptomycin (PAA, Austria), and 10% FBS, fetal bovine serum (Invitrogen) at 37°C in 5% (v/v) CO2 humidified atmosphere. For the co-expression of two different fusion constructs, the molar ratio of the two plasmids was kept at 1:1 calculated from mass and size of the plasmids for transfection.

Electroporation (Bio-Rad, Hercules, CA) was used for transfection of CHO cells. ~90% confluent cells in a flask were washed once with 1×PBS, phosphate buffered saline (BSF, the Biopolis Shared Facilities, SG), trypsinized with 0.25% trypsin-0.03% EDTA solution (BSF) for 5 min at 37°C, and then re-suspended in culture medium. Cells (~1×106) were precipitated by centrifugation and re-suspended in small amount of culture medium in an electroporation cuvette, 2-mm wide. After mixing the DNA for co-transfection, 20 mg in total, with cells, the cuvette(Bio-Rad) was chilled on ice for 5 min. GenePulser Xcell (Bio-Rad) was used for electroporation by following the manufacturer's preprogrammed protocol for CHO cells. After electroporation, cells were left for 10 min at room temperature, and ~50,000 cells/well were seeded in wells of a six-well chamber containing prewashed coverglasses (30 mm in diameter; Lakeside, Monee, IL, USA). Transfected cells grew in the culture medium for 24–36 hrs before measurement.

At the time of observation for FCCS measurements, cells were washed thoroughly with 1×PBS to avoid

influence of media on fluorescence and covered with 1ml 1×PBS in the minichamber during measurements. EGF stock was neutralized by HEPES (50mM, pH7.2, BSF) before addition to the minichamber. The final concentration of EGF (Sigma, St. Louis, MO, USA) for stimulation experiments was kept at 100 ng/ml. To avoid fast internalization of the membrane receptors after EGF activation during SW-FCCS observation, cells were incubated with endocytosis inhibitors 30 minutes before adding EGF. The final concentration of the inhibitors was NaN3 (Sigma), 10 mM; NaF (Sigma), 2 mM; 2-deoxy-D-glucose (Sigma), 5 mM, respectively (8).

3.3. SW-FCCS setup

We used the same instrumentation as described in a previous paper (8). In brief, an Olympus FV 300 confocal microscope was modified and combined with a home-made FCCS attachment: Both fluorescent proteins were excited by an argon ion 514-nm laser (Melles Griot, Albuquerque, NM, USA). The excitation laser was reflected by a 458/514 dichroic mirror and focused to the sample where it formed a confocal volume by a water-immersion objective (60×, NA 1.2; Olympus, JP). The laser power of 20 μW and 30 μW were used for the CHO cells FCCS measurements and confocal image taking, respectively. Emission spectra passed through a 150-μm pinhole and were able to go to two different directions by the help of a home-built slider: the path to the FV300 photomultipliers for imaging and to two avalanche photodiodes (SPCM-AQR-14-FC; Pacer, Berkshire, UK) for FCCS. In the FCCS mode, the fluorescence are splited by a 560DCLP dichroic mirror (Omega Optical, Brattleboro, VT, USA) followed by two band-pass filters, 545AF35 and 615DF45 (Omega Optical), for green and red channels, respectively. The autocorrelation and cross-correlation curves were computed online by a hardware correlator (Flex02-01D; Correlator.com, Bridgewater, NJ, USA).

3.4. SW-FCCS calculation on the fractions of dimers and complexes

The SW-FCCS was previously described (19). In brief, the auto- and cross-correlation function can be written in terms of count per molecule per second of all kinds of proteins involved and their concentrations. Those proteins included EGFR-FP monomer, EGFR-FP dimers, single PTB-EGFP, PTB-EGFP/mRFP-EGFR binding complex, and so on. Quenching and cross-talk were also considered in the functions to eliminate calculation error. The equations include:

The normalized autocorrelation function (ACF) and Cross-correlation function (CCF) is given by (20)

$$G(\tau)=\frac{\langle F(t)\cdot F(t+\tau)\rangle}{\langle F(t)\rangle^2} \quad (1)$$

$$G_x(\tau)=\frac{\langle F_i(t)\cdot F_j(t+\tau)\rangle}{\langle F_i(t)\rangle\langle F_j(t)\rangle} \quad (2)$$

When τ is the lag time. For a molecular species, PTB-EGFP for example, that diffuses freely in three dimensions, the theoretical correlation function is given by (21).

$$G(\tau)=\frac{1}{N}\left(1+\frac{\tau}{\tau_D}\right)\left[1+\frac{\tau}{\tau_D}K^2\right]^{-1/2}+G_\infty \quad (3)$$

Where K=ωz/ω0 (the ratio of height of the focal volume over its waist), and τD=ω0²/4D. But when the single molecular species binds to some other molecule, there will be two particles, whose diffusion times are τD1 and τD2. And we also need to take the triplet state into account, so the correlation function is expressed as:

$$G(\tau)=\frac{1}{N}\left[(1-F_2)\left(1+\frac{\tau}{\tau_{D1}}\right)^{-1}\left(1+\frac{\tau}{\tau_{D1}}K^2\right)^{-1/2}+F_2\left(1+\frac{\tau}{\tau_{D2}}\right)^{-1}\left(1+\frac{\tau}{\tau_{D2}}K^2\right)^{-1/2}\right]\left(1+\frac{F_{trip}e^{-\tau/\tau_{trip}}}{1-F_{trip}}\right)+G_\infty \quad (4)$$

Where Ftrip is the fraction of the particles that have entered the triplet state; and τtrip is the triplet state relaxation time. And for a molecular species, like EGFR-FPs and PMT-FPs, that diffuses in two dimensions the theoretical correlation function is given by (22)

$$G(\tau)=\frac{1}{N}\left(1+\frac{\tau}{\tau_D}\right)^{-1}+G_\infty \quad (5)$$

Because there are always some proteins not locating on the membrane but diffusing near the membrane, and a triplet state of the protein has to be considered, the correlation function is updated into:

$$G(\tau)=\frac{1}{N}\left[(1-F_2)\left(1+\frac{\tau}{\tau_{D1}}\right)^{-1}+F_2\left(1+\frac{\tau}{\tau_{D2}}\right)^{-1}\right]\left(1+\frac{F_{trip}e^{-\tau/\tau_{trip}}}{1-F_{trip}}\right)+G_\infty \quad (6)$$

For Cross-correlation function where we counted in two components but the triplet states won't correlate, the following equation is applied:

$$G(\tau)=\frac{1}{N}\left[(1-F_2)\left(1+\frac{\tau}{\tau_{D1}}\right)^{-1}+F_2\left(1+\frac{\tau}{\tau_{D2}}\right)^{-1}\right]+G_\infty \quad (7)$$

For the quantification of PTB-EGFR binding, we assumed a 1:1 binding stoichiometry, the amplitude of the ACFs and CCF, Gi(0) and Gx(0), equation (9)-(11), can then be expressed as a function of η, the count rate per molecule per second (cpm); Ci, the concentrations of the particles involved; qi, the correction factors accounting for changes in fluorescence yields upon binding via processes such as quenching or fluorescence energy transfer; βi, the uncorrelated background count rate ; NA, the Avogadro's number and Veff, the effective observation volume

obtained from (16, 19, 23)

$$V_{eff} = \pi^{3/2} w_0^{\,2} w_z$$

(8)

$$G_g(0) = \frac{(\eta_g^g)^2 C_g + (\eta_r^g)^2 C_r + (q_g \eta_g^g + q_r \eta_r^g)^2 C_{gr}}{N_A V_{eff} [\eta_g^g C_g + \eta_r^g C_r + (q_g \eta_g^g + q_r \eta_r^g) C_{gr} + \beta^g / (N_A V_{eff})]^2}$$

(9)

$$G_r(0) = \frac{(\eta_g^r)^2 C_g + (\eta_r^r)^2 C_r + (q_g \eta_g^r + q_r \eta_r^r)^2 C_{gr}}{N_A V_{eff} [\eta_g^r C_g + \eta_r^r C_r + (q_g \eta_g^r + q_r \eta_r^r) C_{gr} + \beta^r / (N_A V_{eff})]^2}$$

(10)

$$G_x(0) = \frac{\eta_g^g \eta_g^r C_g + \eta_r^g \eta_r^r C_r + (q_g \eta_g^g + q_r \eta_r^g)(q_g \eta_g^r + q_r \eta_r^r) C_{gr}}{N_A V_{eff} [\eta_g^g C_g + \eta_r^g C_r + (q_g \eta_g^g + q_r \eta_r^g) C_{gr} + \beta^g / (N_A V_{eff})]} \times [\eta_g^r C_g + \eta_r^r C_r + (q_g \eta_g^r + q_r \eta_r^r) C_{gr} + \beta^r / (N_A V_{eff})]^{-1}$$

(11)

where 'i' represents green or red labeled particles when applied. Cgr is the concentration of the complex particles; η_g^g and η_r^g are the cpm of the green and red labeled particles in the green channel respectively; η_g^r and η_r^r are the cpm of green and red labeled particles in the red channel respectively. η of PTB-EGFP is mainly between 900-2100 Hz, η of mRFP-EGFR is mainly between 700-2200 Hz. η of PMT-GFP is mainly between 2000 to 3200 Hz, η of PMT-mRFP is mainly between 1500 to 3200 Hz. η of EGFR-EGFP is mainly between 1500-3000 Hz.

For calculation of the dimer percentage in the EGFR-EGFP/mRFP-EGFR group, things are slightly different because we need to consider the contribution of both heterodimer and homodimer (8), so we got the following equations:

$$G_g(0) = \frac{\left(\eta_g^g\right)^2 C_g + \left(\eta_r^g\right)^2 C_r + \left(\eta_{2g}^g\right)^2 C_{2g} + \left(\eta_{2r}^g\right)^2 C_{2r} + \left(\eta_{gr}^g\right)^2 C_{gr}}{N_A V_{eff} \left[\eta_g^g C_g + \eta_r^g C_r + \eta_{2g}^g C_{2g} + \eta_{2r}^g C_{2r} + \eta_{gr}^g C_{gr} + \beta^g / \left(N_A V_{eff}\right)\right]^2}$$

(12)

$$G_r(0) = \frac{\left(\eta_g^r\right)^2 C_g + \left(\eta_r^r\right)^2 C_r + \left(\eta_{2g}^r\right)^2 C_{2g} + \left(\eta_{2r}^r\right)^2 C_{2r} + \left(\eta_{gr}^r\right)^2 C_{gr}}{N_A V_{eff} \left[\eta_g^r C_g + \eta_r^r C_r + \eta_{2g}^r C_{2g} + \eta_{2r}^r C_{2r} + \eta_{gr}^r C_{gr} + \beta^r / \left(N_A V_{eff}\right)\right]^2}$$

(13)

$$G_x(0) = \frac{\eta_g^g \eta_g^r C_g + \eta_r^g \eta_r^r C_r + \eta_{2g}^g \eta_{2g}^r C_{2g} + \eta_{2r}^g \eta_{2r}^r C_{2r} + \eta_{gr}^g \eta_{gr}^r C_{gr}}{N_A V_{eff} \left[\eta_g^g C_g + \eta_r^g C_r + \eta_{2g}^g C_{2g} + \eta_{2r}^g C_{2r} + \eta_{gr}^g C_{gr} + \beta^g / \left(N_A V_{eff}\right)\right]} \times \left[\eta_g^r C_g + \eta_r^r C_r + \eta_{2g}^r C_{2g} + \eta_{2r}^r C_{2r} + \eta_{gr}^r C_{gr} + \beta^r / \left(N_A V_{eff}\right)\right]^{-1}$$

(14)

Curve fitting was performed by a self-written program in Igor Pro 6.0 (WaveMetrics, Lake Oswego, OR).

The dimer percentage of co-transfected dual-color EGFR is defined as:

$$\frac{2 \times (C_{2g} + C_{2r} + C_{gr})}{C_g + C_r + 2 \times (C_{2g} + C_{2r} + C_{gr})}$$

(15)

The EGFR-PTB binding quantification is derived like this: for the cells different FP expression levels, which is most of cases, the binding percentage is expressed as a function of the total concentration of either the total PTB-EGFP (CG) or total mRFP-EGFR(CR) molecules:

$$\frac{C_{GR}}{C_G + C_{GR}} \times 100 \quad \text{or} \quad \frac{C_{GR}}{C_R + C_{GR}} \times 100$$

(16)

which is larger, because the number of complexes is limited by the number of lower concentrated molecules (16). And the cells we picked always expressed those two molecules differing no more than a factor of 2 observed from the focus.

The binding quantification, complex percentage for PTB-EGFR interaction, and dimer percentage for EGFR-EGFR dimerization, were calculated by a self-written program in Mathematica 5 (Wolfram Research, Champaign, IL).

4. RESULT

4.1. Calibration for Fluorescence Correlation and Cross-Correlation Spectroscopy (FCS and FCCS)

All our measurements are performed on CHO cells, either on the membrane or in the cytoplasm. We first calibrated the FCS system with a standard fluorophore, Rhodamine 6G, with an diffusion coefficient D of 426 $\mu m^2/s$ (24). At an excitation wavelength of 514 nm and a laser power of 20 μW, the value of □D was 39.2 ± 3.2 μs, the structure factor K was 6.25 ± 1.17, and the convergence value for long time G∞ deviated from the expected value of 1 by less than 1.1 % in all measurements. The structure factor was fixed for all further measurements. Next we proceeded to determine the diffusion coefficients of all constructs within CHO cells. For experiments only those cells were chosen which have similar expression levels of green and red fluorescent protein (FP) labeled molecules. All measurements were performed on the upper plasma membrane above the nucleus where the membrane is parallel to the xy focal plane of the instrument and is unhindered by interactions with any surfaces (25, 26). The excitation wavelength for these measurements was 514 nm at a laser power of 20 μW before the objective. The constructs show a clear difference in the measured values of D depending on their expected localization and thus the expected viscosity of their local environment (Table 1). Cytoplasmic proteins (PTB-EGFP) showed values of D on the order of ~20-30 $\mu m^2/s$. Membrane bound proteins (PMT-FPs) had a D of ~0.7$\mu m^2/s$ and transmembrane proteins (EGFR-FPs) showed diffusion coefficients on the order of ~0.3$\mu m^2/s$. These differences are within the

Table 1. Diffusion coefficients of the green and red autocorrelation function (ACF_G and ACF_R) and the cross-correlation function (CCF) measured for different combinations of proteins co-expressed in CHO cells

Proteins	D [$\mu m^2/s$] ACF_G	D [$\mu m^2/s$] ACF_R	D [$\mu m^2/s$] CCF	N
PMT-GFP/PMT-mRFP (neg. ctrl)	0.4 ± 0.2	0.3 ± 0.1	1.0±0.5	82
EGFR-EGFP/mRFP-EGFR	0.3 ± 0.2	0.3 ± 0.2	0.5±0.3	65
PTB-EGFP/mRFP-EGFR (- *EGF*)	23 ± 12 (0.7 ± 0.5)	0.3 ± 0.2	22±12 (0.6±0.4)	19
PTB-EGFP/mRFP-EGFR (+*EGF 20min*)	23 ± 12 (1.3 ± 1.1)	0.3 ± 0.2	25±15 (0.7±0.5)	19
PTB-EGFP/PMT-mRFP (-*EGF*)	28 ± 10 (1.0±0.5)	0.8 ± 0.5	30±20 (0.7±0.5)	12
PTB-EGFP/PMT-mRFP (+*EGF 20min*)	31 ± 10 (0.8±0.7)	0.7 ± 0.3	27±14 (1.0±0.5)	12
mRFP-EGFR-EGFP (pos. ctrl)	0.8 ± 0.3	0.7 ± 0.3	0.3±0.2	25

Values in parenthesis represent a second, slower diffusion coefficient if present. N represents the number of measurements performed for each case. The values have been calibrated against Rhodamine 6G with an assumed diffusion coefficient of 426 $\mu m^2/s$.

expectation of membranes having a two order of magnitude higher viscosity than aqueous solution or the cytoplasm (27).

It should be noted that the correlation curves for PTB-EGFP showed a small slower moving fraction (detected in 69 % of the cases, with a fraction of about 8% of the total) with a diffusion coefficient of ~0.7 $\mu m^2/s$. This indicated that possibly even in the basal non-stimulated state some PTB-EGFP is bound to the membrane which implies some basal phosphorylation of the EGFR.

4.2. Z-scan

FCS measurements were performed in the z-direction across the upper plasma membrane of CHO cells (25, 28, 29). We chose different points along the z-direction by moving the focus across the membrane and measuring diffusion coefficients in the cytoplasm on the membrane and outside the cell. The ACF curves suggested different diffusion behaviour for the different constructs at different locations. All measurements outside the cell did not show any correlations as expected since proteins are expressed only on the membrane and in the cytoplasm. For PTB-EGFP, measurements in the cytoplasm showed the typical diffusion coefficient already shown in Table 1. For PMT little correlation is detected in the cytoplasm. For EGFR correlations are seen in the cytoplasm, especially when no internalization inhibitors are applied, with a slow diffusion time of 308 ± 141 µs. We attribute this to either internalized mRFP-EGFR or possibly mRFP-EGFR which is transported from the ER to the plasma membrane. However, in the vicinity of the membrane we see a strong dependence of the ACF curves on the position of the focal volume. In Figure 1 we show the ACFs collected on the membrane, 0.4 µm and 1.4 µm below the membrane. mRFP-EGFR exhibits one slow diffusion coefficient and only the amplitude of the ACF is influenced by the position. In contrast, for PTB-EGFP measurements we see a fast and slow component of the diffusion coefficient. The fast diffusion coefficient is the same within the margins of error as the one measured in the cytosol. The slow diffusion coefficient is similar to the diffusion coefficient measured for the mRFP-EGFR on the plasma membrane. The nearer to the membrane, the more the slow component, i.e. the component with the EGFR-like diffusion coefficient, contributes to the ACF. Since the half-height of the focal volume is no larger than 1.4 µm, we measure the diffusion below the membrane (-1.4 µm) and found that there is no slow diffusing component for PTB-EGFP, indicating that PTB-EGFP freely diffuses in the cytoplasm.

Closer to the membrane PTB-EGFP shows some slow diffusing component with a fraction of 8 ± 2 % (mean ± standard error of the mean (SEM)) for PTB-EGFP/PMT-mRFP. This indicates either some basic binding, which is not EGFR-specific, of PTB-EGFP to membrane proteins or some FCS artefact as has been found before (30). In any case this defines the lowest value of membrane binding we can detect for PTB-EGFP in our assays.

4.3. SW-FCCS Control measurements

To set the stage for the measurement of interactions we have measured negative controls between differently labeled plasma membrane targeting proteins (PMT) and phosphotyrosine binding domain (PTB). The negative controls give low cross-correlations with interaction percentages of 4 ± 1 % (average ± standard error of the mean (SEM)) for PTB-EGFP/PMT-mRFP. It should be noted that many of the negative controls don't give any solution for the interaction percentage and thus this estimate is a conservative upper bound. The positive control (mRFP-EGFR-EGFP) gave a much higher cross-correlation amplitude with a maximum interaction percentage of 48 ± 3 %. These values define the dynamic range achievable by SW-FCCS in these measurements. The reasons that not 100% cross-correlation can be achieved are at least threefold. Firstly, the detection volumes will not be exactly equal due to the different emission wavelength detected for the two proteins. Secondly, not all fluorescent proteins are in a fluorescent state but can be in dark states. This has been shown in particular for the red fluorescent proteins (31). And thirdly, especially the red fluorescent proteins suffer from photobleaching. As a first test we repeated measurements of the dimerization of the EGFR in the absence of stimulation (Figure 2). The values for the interaction percentage were 32 ± 3 % for EGFR-EGFP/mRFP-EGFR. When set in relation to the maximum percentage of the positive control, this implies a percentage of about 67% of all receptors being in dimers (see Table 2), which is the same value as measured in an earlier study (8).

4.4. The interaction of PTB and EGFR

Having set the bottom and upper limit for the EGFP and mRFP pair under the presented conditions, the interaction between proteins can be quantified. For measurements with and without EGF stimulation we used internalization inhibitors to avoid the rapid internalization of EGFR which would make the interaction percentage

Table 2. Interaction percentages of different co-transfected proteins as determined by SW-FCCS

	Complex% (±SE)	Normalized Complex% (±SE)	N
PMT-EGFP/PMT-mRFP (neg. ctrl)	4±1	8±1	82
EGFR-EGFP/mRFP-EGFR(dimer %)	32±3	67±6	65
PTB-EGFP/mRFP-EGFR (*-EGF*)	13±3	26±6	19
PTB-EGFP/mRFP-EGFR (*+EGF 20min*)	22±4	45±8	18
PTB-EGFP/PMT-mRFP (*-EGF*)	5±2	9±3	12
PTB-EGFP/PMT-mRFP (*+EGF 20min*)	5±2	9±3	10
mRFP-EGFR-EGFP (pos. ctrl)	48±3	100±6	25

For EGFR-EGFP/mRFP-EGFR, the complex percentage represents the dimer percentage. SE is the standard error of the mean and N the number of independent measurements performed. In the second column the percentages have been normalized to the value of the positive control.

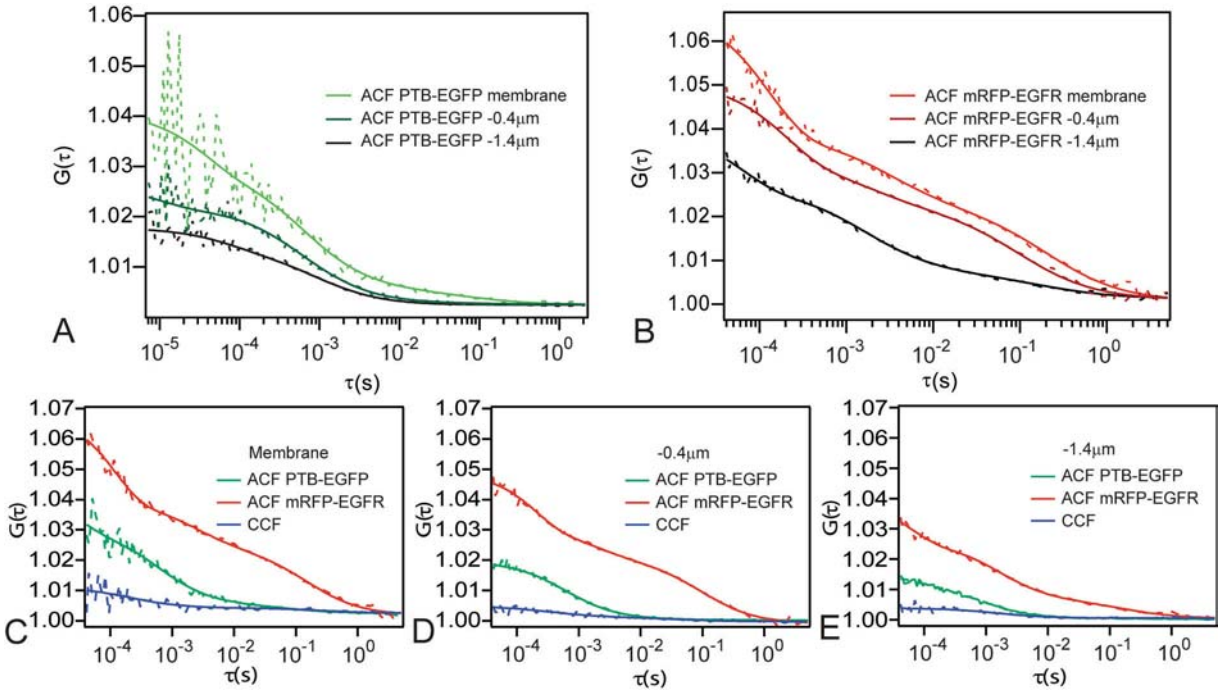

Figure 1. FCCS z-scans for PTB-EGFP/mRFP-EGFR co-transfected CHO cells around the upper membrane in the absence of stimulation. The z-scans were performed at 3 heights, on the membrane, 0.4 μm below the membrane and 1.4 μm below the membrane, suggesting different diffusion behaviour for the different constructs at different locations. (A) ACF curves of PTB-EGFP: two diffusive components exist in the curves; one is on the order of cytosolic proteins and another is consistent with EGFR-FPs diffusion on the membrane. (B) ACF curves of mRFP-EGFR. The amplitude of the ACF is influenced by the focal position in relation to the membrane. (C), (D), and (E): ACF and CCF curves of PTB-EGFP/mRFP-EGFR at different locations.

measurements very difficult and imprecise. We measured the cross-correlation on a single cell before and after the addition of 100 ng/ml EGF by focusing on a single position. For consistency we used the peak intensity in the red channel as the membrane position and refocused on the membrane before every measurement to avoid artifacts of membrane movement. After addition we took several measurements at different times ranging from 3 minutes to about 30 minutes after EGF addition.

The amplitudes of cross-correlation curves measured before stimulation from cells co-expressing PTB-EGFP/mRFP-EGFR (13 ± 3 %) were much higher than those expected for pure cross talk (Figure 3). In addition they were as well higher than the negative control (5 ± 2 %). This indicates that there is some basic binding of PTB-EGFP to mRFP-EGFR even in the absence of stimulation. This is probably due to a low basal amount of phosphorylated EGFR even when the cells are not stimulated. After 20 minutes stimulation with EGF the interaction percentage increased to 22 ± 4 % showing a statistically significant increase in PTB-EGFP binding. It should be noted here that the SEM is somewhat larger than for the other measurements which is due to the fact that the values before and after stimulation can vary over a larger range than seen for the negative and positive controls. This is a reflection of the biological variability between cells (Figure 4). However, independent of the initial value of the interaction percentage before stimulation, the interaction percentage increased mainly in the first 5 minutes after stimulation for 16 out of 21 cells and showed a slower increase at 20 minutes after stimulation. In the negative control of PTB-EGFP/PMT-mRFP in which we stimulated cells with EGF, the percentage shows no significant increase with time (5 ± 2 % at 20 min) and is markedly below the level when mRFP-EGFR is co-expressed. We

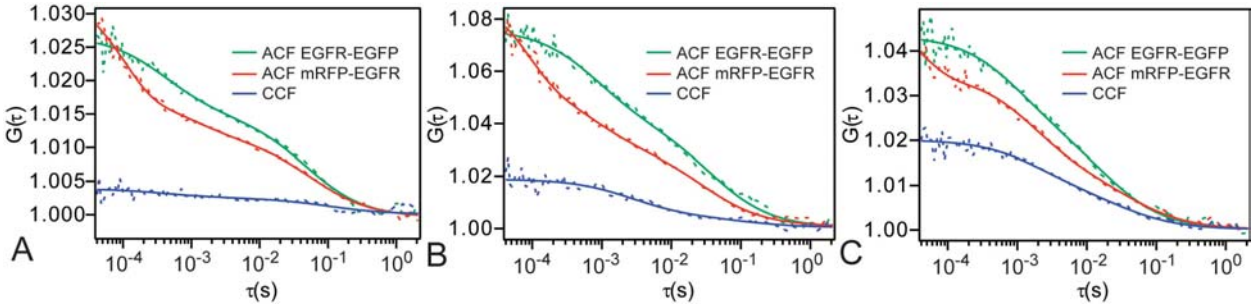

Figure 2. EGFR-EGFP/mRFP-EGFR form dimers in the absence of stimulation. The normalized value of dimer percentage is 67 ± 6 %. Graph A, B and C present the various levels of dimer percentage detected.

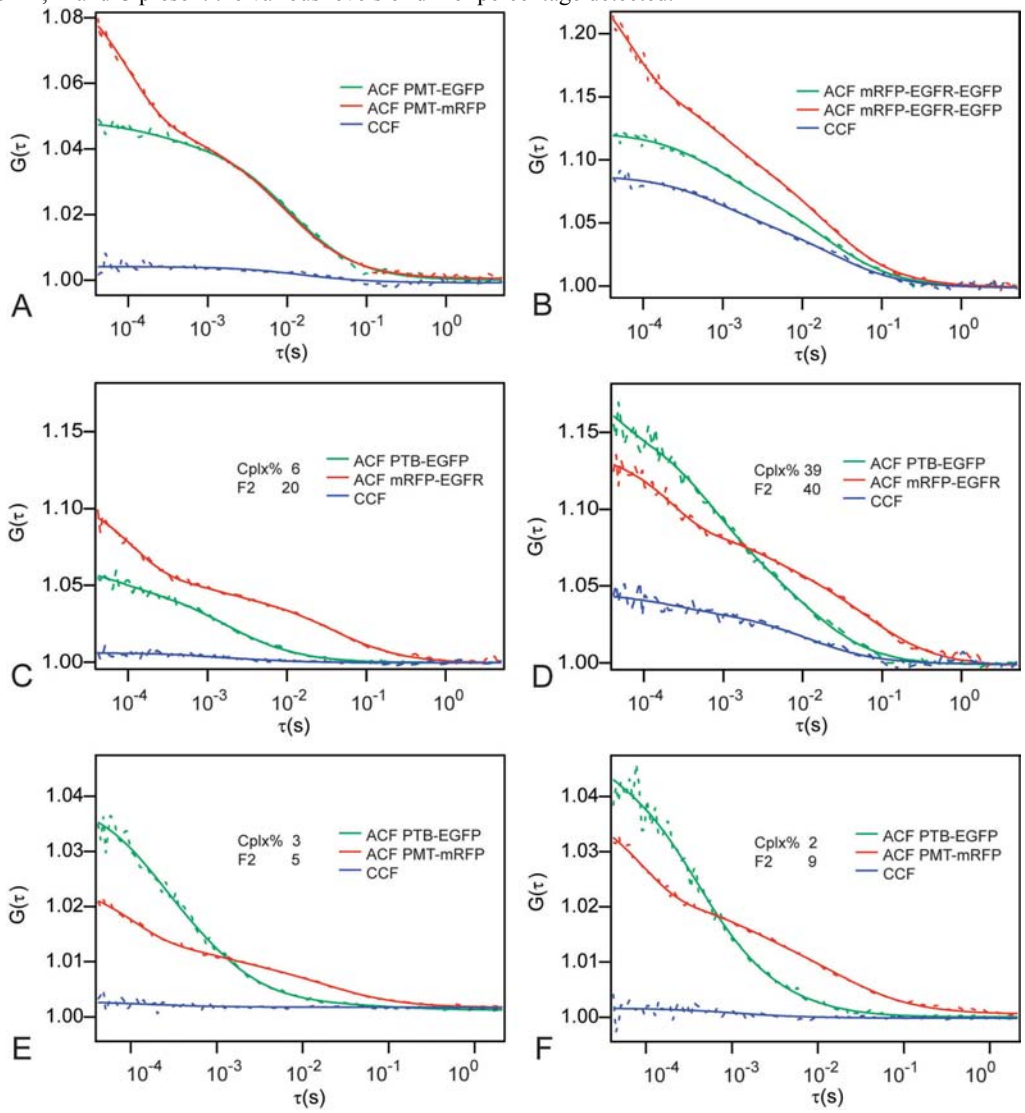

Figure 3. Auto- and cross-correlation curves of controls and experiment. The colors of the FP labels are indicated by the colors of the curves. (A) PMT-EGFP/mRFP (negative control) shows the lowest level of cross-correlations. (B) mRFP-EGFR-EGFP (positive control) showing the highest level of cross-correlation for our system. (C) and (D) PTB-EGFP/mRFP-EGFR before and after 20 min of stimulation, respectively, indicating not only the increase of the amplitude of the CCF but also an increase of the slow diffusing component of the CCF. (E) and (F) PTB-EGFP/PMT-mRFP before and after 20 min of stimulation (negative control) shows no significant increase in complex percentage. F_2 stands for fraction of the slow component in the CCF. Cplx % stands for the complex percentage as determined from the CCF amplitude (not normalized).

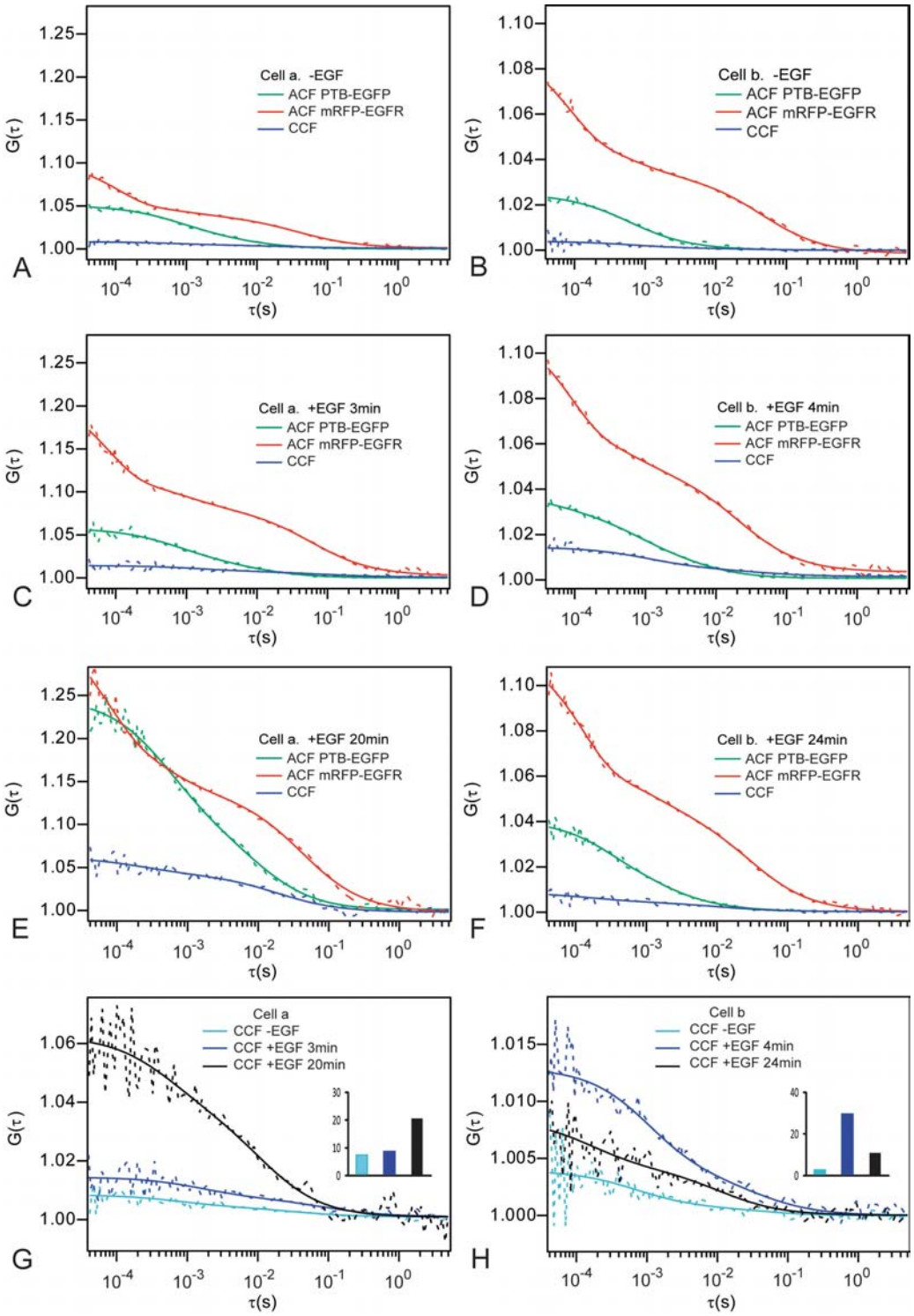

Figure 4. Dynamic changes of PTB-EGFP/mRFP-EGFR interaction exhibit cell dependent patterns, which contributes to the large variability of the complex percentage measured. (A, B): before EGF stimulation. (C, D): after a short exposure of EGF. (E, F): PTB-EGFP/mRFP-EGFR after a long exposure of EGF. (G, H): Comparison of CCF curves for two different cells showing different activation patterns. Although in both cases binding can be clearly detected by a rise in the second slower diffusing component (similar to EGFR-FP) in the CCF, the time of highest interaction is different for the two cells. The complex percentages are shown as a time-course column chart: the colors of the column indicate the time coinciding with the CCF curves, and the Y-axis values present the complex percentage values (not normalized).

should note here that some cells (3 in 19) internalize mRFP-EGFR very rapidly even in the presence of internalization inhibitors. We excluded these cells from our evaluations since they show clearly faster diffusion times and higher CCF amplitudes, possibly due to the presence of multiple EGFR/PTB pairs in vesicles below the membrane.

To further prove that the interaction between mRFP-EGFR and PTB-EGFP is driven by EGF stimulation we observed also the fraction of the slow diffusing component of PTB-EGFP in the ACF. This should rise when more PTB-EGFP binds to mRFP-EGFR in the plasma membrane as is indeed found in our experiments (Figure 3). Comparing the interaction percentage found in the CCF and the fraction of the slower diffusing component of the ACF, we see the same trends of increasing values for both numbers in 14 out of 18 cells. The absolute values of the two numbers are not comparable though, since the first represents the percentage of interacting mRFP-EGFR and PTB-EGFP while the second describes how many of the total PTB-EGFP seen is membrane bound. However, the same trend observed in both values is consistent with an increased binding of PTB-EGFP to mRFP-EGFR on the membrane after EGF stimulation.

5. DICUSSION

We have presented here the quantitative measurement in space and time of the interaction of EGFR with a phosphotyrosine binding domain (PTB) in live cells using SW-FCCS. This is, to our knowledge, the first time-dependent quantitative study of a cytosolic protein binding to a membrane receptor in an activation dependent manner by SW-FCCS. SW-FCCS was to date only used to study the interaction between membrane proteins or cytosolic proteins. The measurements presented here demonstrate that SW-FCCS can also be used to study the binding of cytosolic proteins to membrane proteins despite the fact that this type of experiment poses particular problems. Firstly, there is a mismatch in concentrations between the cytosolic and membrane proteins leading to a limited response in the cross-correlation amplitudes. Secondly, binding is activation dependent and thus has to be observed over time, posing problems of membrane focusing. And thirdly, because of the necessary EGF stimulation only one measurement can be performed per cell or even cell chamber. In combination with the variability of the biological response of different cells this makes measurements difficult.

Our findings indicate that there is little non-specific binding of PTB-EGFP (<12 %, normalized percentage to positive control) to membranes lacking mRFP-EGFR independent of EGF stimulation. However, in the absence of stimulation, EGFR expressing cells showed a somewhat higher percentage of PTB-EGFP binding (~ 26 %) to the plasma membrane than cells which lacked EGFR. This indicated that even in the non-stimulated state some PTB-EGFP is interacting with mRFP-EGFR, implying a low level of mRFP-EGFR phosphorylation. The basal phosphorylation for mRFP-EGFR has been observed by our group previously, see Figure 2A in (8). Upon activation, PTB-EGFP is recruited to the membrane within minutes although the full binding is seen only at a later stage about 20-30 minutes in the presence of EGF (~ 45 %). This finding is supported also by the fact that the cross-correlation function (CCF) shows an increasing fraction of slowly diffusing, i.e. membrane bound, PTB-EGFP compared to the fast cytosolic fraction which diffuses almost a factor 50-70 faster. It should be noted though that, as already reported in our earlier work, we sometimes recorded very big intensity fluctuations in combination with a smaller diffusion coefficient. We interpret this as receptor clustering on the membrane. The observed increase in the diffusion time implies very large receptor clusters since the diffusion coefficient is only weakly dependent on particle size in membranes (32). Although large clusters can be easily identified, smaller clusters may be difficult to detect especially if they constitute a small portion of a measurement. This might partly explain the variability in results between cells. It would be very interesting to use Photon Counting histogram (33) and Fluorescence Distribution Analysis (11, 34, 35), or to determine distribution of brightness of these clusters in future measurements.

This study shows that EGFR activation, and indirectly phosphorylation, can be followed in time by SW-FCCS in live cell. With previous measurements we have demonstrated now that various interactions between membrane proteins, between cytosolic proteins, and now between cytosolic and membrane proteins can be followed in a quantitative manner by SW-FCCS. This opens the possibility to quantitatively investigate the interactions in a complete signal transduction pathway in live cells or possibly organisms in the future.

6. ACKNOWLEDGEMENTS

The authors thank Dr. Philippe I. H. Bastiaens for the PTB plasmid. The authors gratefully acknowledge Mr. Yong Hwee Foo for help with the SW-FCCS analysis as well as the technical support and Dr. Thankiah Sudhaharan for the help with cell cultures. This work was supported in part by a grant from the Biomedical Research Council of Singapore (07/1/21/19/488, R-143-000-351-305) to T.W. and S.A. X.M. is a recipient of a scholarship from a grant of the Ministry of Education of Singapore (R-143-000-358-112).

7. REFERENCES

1. Antony W. Burgess: EGFR family: structure physiology signalling and therapeutic targets. *Growth Factors* 26, 263-274 (2008)

2. Fortunato Ciardiello, Giampaolo Tortora: EGFR antagonists in cancer treatment. *N Engl J Med* 358, 1160-1174 (2008)

3. Kathryn M. Ferguson: Structure-based view of epidermal growth factor receptor regulation. *Annu Rev Biophys* 37, 353-373 (2008)

4. Nancy E. Hynes, Heidi A. Lane: ERBB receptors and

cancer: the complexity of targeted inhibitors. *Nat Rev Cancer* 5, 341-354 (2005)

5. H. Michael Shepard, Cathleen M Brdlik, Hans Schreiber: Signal integration: a framework for understanding the efficacy of therapeutics targeting the human EGFR family. *J Clin Invest* 118, 3574-3581 (2008)

6. Ami Citri, Yosef Yarden: EGF-ERBB signalling: towards the systems level. *Nat Rev Mol Cell Biol* 7, 505-516 (2006)

7. Peter J. Verveer, Fred S. Wouters, Andrew R Reynolds, Philippe I H Bastiaens: Quantitative imaging of lateral ErbB1 receptor signal propagation in the plasma membrane. *Science* 290, 1567-1570 (2000)

8. Ping Liu, Thankiah Sudhaharan, Rosita M. L. Koh, Ling C. Hwang, Sohail Ahmed, Ichiro N. Maruyama, Thorsten Wohland: Investigation of the dimerization of proteins from the epidermal growth factor receptor family by single wavelength fluorescence cross-correlation spectroscopy. *Biophys J* 93, 684-698 (2007)

9. Andrew H. A. Clayton, Suzanne G. Orchard, Edouard C. Nice, Richard G. Posner, Antony W. Burgess: Predominance of activated EGFR higher-order oligomers on the cell surface. *Growth Factors* 26, 316-324 (2008)

10. Takanori Moriki, Hiroko Maruyama, Ichi N. Maruyama: Activation of preformed EGF receptor dimers by ligand-induced rotation of the transmembrane domain. *J Mol Biol* 311, 1011-1026 (2001)

11. Saveez Saffarian, Yu Li, Elliot L. Elson, Linda J. Pike: Oligomerization of the EGF receptor investigated by live cell fluorescence intensity distribution analysis. *Biophys J* 93, 1021-1031 (2007)

12. Kirsten Bacia, Sally A. Kim, Petra Schwille: Fluorescence cross-correlation spectroscopy in living cells. *Nat Methods* 3, 83-89 (2006)

13. Kenta Saito, Ikuo Wada, Mamoru Tamura, Masataka Kinjo: Direct detection of caspase-3 activation in single live cells by cross-correlation analysis. *Biochem Biophys Res Commun* 324, 849-854 (2004)

14. Roger Y. Tsien: The green fluorescent protein. *Annu Rev Biochem* 67, 509-544 (1998)

15. Robert E. Campbell, Oded Tour, Amy E. Palmer, Paul A. Steinbach, Geoffrey S. Baird, David A. Zacharias, Roger Y. Tsien: A monomeric red fluorescent protein. *Proc Natl Acad Sci U S A* 99, 7877-7882 (2002)

16. Xianke Shi, Yong Hwee Foo, Thankiah Sudhaharan, Shang-Wei Chong, Vladimir Korzh, Sohail Ahmed, Thorsten Wohland: Determination of dissociation constants in living zebrafish embryos with single wavelength fluorescence cross-correlation spectroscopy. *Biophys J* 97, 678-686 (2009)

17. Thankiah Sudhaharan, Ping Liu, Yong Hwee Foo, Wenyu Bu, Kim Buay Lim, Thorsten Wohland, Sohail Ahmed: Determination of *in vivo* dissociation constant, KD, of Cdc42-effector complexes in live mammalian cells using single wavelength fluorescence cross-correlation spectroscopy. *J Biol Chem* 284, 13602-13609 (2009)

18. Martin Offterdinger, Virginie Georget, Andreas Girod, Philippe I. H. Bastiaens: Imaging phosphorylation dynamics of the epidermal growth factor receptor. *J Biol Chem* 279, 36972-36981 (2004)

19. Ling Chin Hwang, Thorsten Wohland: Dual-color fluorescence cross-correlation spectroscopy using single laser wavelength excitation. *Chemphyschem* 5, 549-551 (2004)

20. Douglas Magde, Elliot Elson, and W. W. Webb: Thermodynamic Fluctuations in a Reacting System—Measurement by Fluorescence Correlation Spectroscopy. *Phys Rev Lett* 29, 705-708 (1972)

21. Jerker Widengren, Rudolf Rigler, Ülo Mets: Photodynamic properties of green fluorescent proteins investigated by fluorescence correlation spectroscopy. *J Fluoresc* 4, 255-258 (1994)

22. Elliot L. Elson, Douglas Magde: Fluorescence correlation spectroscopy. I. Conceptual basis and theory. *Biopolymers* 13, 1-27 (1974)

23. Petra Schwille, Franz-Josef Meyer-Almes, Rudolf Rigler: Dual-color fluorescence cross-correlation spectroscopy for multicomponent diffusional analysis in solution. *Biophys J* 72, 1878-1886 (1997)

24. Zdenek Petrasek, Petra Schwille: Precise measurement of diffusion coefficients using scanning fluorescence correlation spectroscopy. *Biophys J* 94, 1437-1448 (2008)

25. A. Benda, M. Benes, V. Marecek, A. Lhotsky, W. T. Hermens, M. Hof: How to determine diffusion coefficients in planar phospholipid systems by confocal fluorescence correlation spectroscopy. *Langmuir* 19, 4120-4126 (2003)

26. S. Milon, R. Hovius, H. Vogel and T. Wohland: Factors influencing fluorescence correlation spectroscopy measurements on membranes: simulations and experiments. *Chem Phys* 288, 171-186 (2003)

27. Harvey Lodish, Arnold Berk, Paul Matsudaira, Chris A. Kaiser, Monty Krieger, Matthew P. Scott, Lawrence Zipursky, James Darnell: Biomembranes and cell architecture. In: Molecular Cell Biology. *W.H.Freeman & Co Ltd*, NY (2003)

28. Thomas Dertinger, Iris von der Hocht, Aleš Benda, Martin Hof, Jörg Enderlein: Surface sticking and lateral diffusion of lipids in supported bilayers. *Langmuir* 22, 9339-9344 (2006)

29. Magdalena Przybylo, Jan Sýkora, Jana Humpolí ková,

Aleš Benda, Anna Zan, Martin Hof: Lipid diffusion in giant unilamellar vesicles is more than 2 times faster than in supported phospholipid bilayers under identical conditions. *Langmuir* 22, 9096-9099 (2006)

30. Cécile Fradin, Asmahan Abu-Arish, Rony Granek, Michael Elbaum: Fluorescence correlation spectroscopy close to a fluctuating membrane. *Biophys J* 84, 2005-2020 (2003)

31. Lindsey N. Hillesheim**,** Yan Chen**,** Joachim D. Mülle: Dual-color photon counting histogram analysis of mRFP1 and EGFP in living cells. *Biophys J* 91, 4273-4284 (2006)

32. P. G. Saffman, M. Delbruck: Brownian motion in biological membranes. *Proc Natl Acad Sci U S A* 72, 3111-3113 (1975)

33. Yan Chen, Joachim D. Müller, QiaoQiao Ruan**,** Enrico Gratton: Molecular brightness characterization of EGFP *in vivo* by fluorescence fluctuation spectroscopy. *Biophys J* 82, 133-144 (2002)

34. Peet Kask, Kaupo Palo, Nicolas Fay, Leif Brand, Ülo Mets, Dirk Ullmann, Joern Jungmann, Johannes Pschorr, Karsten Gall: Two-dimensional fluorescence intensity distribution analysis: theory and applications. *Biophys J* 78, 1703-1713 (2000)

35. Peet Kask, Kaupo Palo, Dirk Ullmann, Karsten Gall: Fluorescence-intensity distribution analysis and its application in biomolecular detection technology. *Proc Natl Acad Sci U S A* 96, 13756-13761 (1999)

Abbreviations: SW-FCCS: Single wavelength fluorescence cross-correlation spectroscopy, EGFR: epidermal growth factor (EGF) receptor, PTB: phosphotyrosine binding (domain), FCCS: Fluorescence Cross-Correlation Spectroscopy, GFP: green fluorescent protein , mRFP: monomeric red fluorescent protein , PMT: plasma membrane target (sequence), CHO: CHO-K1 (Chinese hamster ovary) cells, ACF: autocorrelation function, CCF: Cross-correlation function, SEM: standard error of the mean, cpm: count rate per molecule per second

Key Words: Epidermal Growth Factor Receptor, Tyrosine Kinase, Phosphotyrosine Binding Domain, FCS, FCCS, SW-FCCS

Send correspondence to: Thorsten Wohland, Department of Chemistry, National University of Singapore, 3 Science Drive 3 Singapore 117543, Singapore, Tel: 65-6516-1248, Fax: 65-6779-1691, E-mail: chmwt@nus.edu.sg